

## Clustering behavior of oscillator arrays

Larry Fabiny and Kurt Wiesenfeld

*School of Physics, Georgia Institute of Technology, Atlanta, Georgia 30332*

(Received 11 June 1990; revised manuscript received 12 November 1990)

We consider the time-periodic behavior of oscillator arrays subject to global coupling. Results are presented for experiments on an electrical circuit comprised of  $p$ - $n$  diode junctions, as well as numerical simulations of an array of iterative maps. In the vicinity of a single-element period-doubling bifurcation, a large number of periodic attractors coexist, differing by the degree of synchronization of the array. Certain general features of the observed dynamical behavior can be understood using a combination of stability analysis, symmetry considerations, combinatorics, and relative sizes of the basins of attraction.

### I. INTRODUCTION

The study of single nonlinear oscillators is a mature field. In contrast, far less is known about the behavior of systems of coupled nonlinear oscillators, though the body of work on the subject is growing rapidly. As a general proposition, one expects that systems consisting of many elements—viewed as a class—will exhibit a far greater variety and complexity of behavior than their single-element counterparts. The hope is that this complexity is not limitless, but rather can be made sense of using a few unifying concepts.

Broadly speaking, there are two ways of mounting an attack on systems consisting of  $N$  oscillators. The first is to consider very small numbers of interacting elements ( $N=2$  or  $3$ ), with the goal of characterizing the complex dynamics (bifurcations, routes to chaos, etc.) that emerge as a function of the control parameters.<sup>1–8</sup> The second approach is to jump immediately to the case of very large  $N$ ,<sup>9–28</sup> with the hope of achieving some sort of (presumably statistical) picture of emerging structures. In this paper, we take this latter approach.

There is presently no general framework for understanding large- $N$  systems. Indeed, it is difficult to see how the geometric insights that help one understand the single oscillator problem—whose dynamics take place in a low-dimensional phase space—can be extended to suit dynamical systems whose phase-space dynamics are high dimensional. Despite the lack of unifying concepts, a number of interesting phenomena have been reported in the literature. These include space-time intermittency,<sup>11,24</sup> phase transitions in stimulated activation networks,<sup>9</sup> phase organization,<sup>16</sup> attractor crowding,<sup>27,28</sup> and self-organized criticality.<sup>29–31</sup> Also worth noting is Huberman's "computing crystal," which mimics certain features of associative memory and learning;<sup>32,33</sup> this work represents a fascinating *application* of fundamental concepts from dissipative dynamical systems with many degrees of freedom. For the most part, the descriptions of these phenomena are at the level of analogies, drawn either from other fields (most often condensed-matter physics), or from archetypical low-dimensional dynamical systems.

In addition, Kaneko has reported extensively on the phenomenology of coupled arrays of chaotic iterative maps,<sup>34</sup> including a description of the hierarchical organization of attractors in phase space. For single attractors, he introduces the notion of "clustering," which refers to the way the array of oscillators partitions into dynamically coherent subsystems. Clustering is a natural concept for many degree of freedom systems, and is also central to the present work. As in Ref. 34, we study *globally coupled* oscillator arrays, though in a parameter regime far from any chaotic dynamics.

A feature often encountered in the study of large- $N$  problems is the presence of large numbers of coexisting attractors in the phase space. For example, this occurs in models of charge-density waves,<sup>15,16</sup> Josephson-junction arrays,<sup>26–28</sup> semiconductor laser arrays,<sup>17</sup> and multimode lasers,<sup>35,36</sup> as well as the computing crystal.<sup>32,33</sup> Such situations may also arise when the underlying equations possess a high symmetry.<sup>37,38</sup> To understand such multistable systems, one is lead naturally to a statistical description, an idea we pursue in this paper.

Though the above motivations are general, the scope of the present work is quite specific. In particular, we present a combination of experimental and numerical results for a system of globally coupled nonlinear oscillators. Experimentally, we study a driven electrical circuit consisting of up to four diode elements, in which we can directly control the magnitude of coupling between the degrees of freedom, near the onset of a period-doubling bifurcation. Our interest in this case is that, for a system of  $N$  elements, there is a large number of coexisting attractors (of order  $2^N$ ). Theoretically, we find that a set of coupled iterative maps gives a good accounting of the experimental results. This agreement leads us to study numerically the case of real interest, namely arrays of many oscillators. We find that the structure of a large number of coexisting attractors, together with simple combinatoric arguments, can account for the *statistical* dynamical behavior of the system in the presence of external random noise.

Although we focus on a relatively narrow range of circumstances in this paper, our ultimate goal is to gain some general understanding of the behavior of  $N$  globally

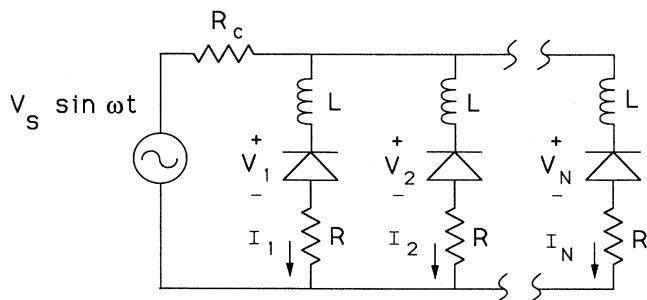


FIG. 1. Experimental realization of a globally coupled oscillator array. The diodes are Motorola MR1122,  $L = 680 \mu\text{H}$ ,  $\omega = 2.25 \times 10^6 \text{ sec}^{-1}$ , and  $R = 143 \Omega$ . This value of  $R$  includes the inductor dc resistance.

coupled oscillators. However, since our theoretical description relies on coupled iterative maps, it is important to make direct contact with more obviously realistic systems. This connection is provided by the diode array (see Fig. 1). This circuit has been well characterized in its single oscillator form.<sup>39-41</sup> It consists of a  $p$ - $n$  junction diode, an inductor, and a resistor connected in series with a sinusoidal voltage source. One can construct a globally coupled system of oscillators by connecting any number  $N$  of these diode-inductor-resistor resonators in parallel and placing this network in series with a coupling resistor. The series resistor plays the important role of coupling the current in any one branch with the currents in all of the other branches.

The contents of this paper are as follows. In Sec. II we introduce the model map equations, whose form is appropriate near a period-doubling bifurcation point. A stability analysis of the map array is performed in Sec. III; one finds that there are some  $2^N$  distinct attractors, which are naturally classified according to their symmetry type. The stability calculation is checked against numerical simulations. In addition to the straightforward issue of stability boundaries, we consider a different, *statistical* characterization in Sec. IV. This measure, which is perhaps more appropriate when dealing with large- $N$  systems, concerns the probability of finding the system in a particular “macroscopic” state, irrespective of the oscillator-by-oscillator details which determine a specific attractor. In Sec. V we turn to experimental measurements on the circuit depicted in Fig. 1, and make comparisons with the behavior of the iterative map array in Sec. VI. Section VII provides a summary of our findings and conclusions.

## II. MODEL MAP EQUATIONS

In an effort to analyze arrays like that in Fig. 1 in a relatively simple way, we begin by considering a set of coupled iterative maps of the form

$$x_k \rightarrow f(x_k; \alpha) + \lambda g(x_1, \dots, x_N), \quad k = 1, \dots, N. \quad (1)$$

Now, in general, one cannot expect that a set of coupled ordinary differential equations—such as the ones describing realistic physical systems like the circuit array—will

be “reducible” to a corresponding set of coupled iterative maps. [Rather, there is a natural connection between the flow in  $M$ -dimensional phase space and an  $(M-1)$ -dimensional iterative map. The reduction of the sort implied by the above equation is from an  $M$ -dimensional flow to a  $(M-N)$ -dimensional map.] Nevertheless, for the purposes of the present study, we are motivated to take the map array seriously, based on the following picture. First, we have a set of  $N$  identical elements—in our experiment these are  $p$ - $n$  junctions—which depend on an external control parameter, which we call the *local stress* parameter. Second, we have direct control of a parameter which governs the *coupling* between the degrees of freedom—this is the resistor in series with the junction array—so that  $\lambda=0$  corresponds to the uncoupled problem. Now, in the uncoupled case, we can imagine studying the Poincaré return map of each oscillator separately, and of course in this limit the dynamics will be captured correctly by the map array. As the coupling parameter is varied away from zero, we anticipate the effect to correspond to a simple perturbation of the “individual” maps.

It is in this spirit that we consider a map array as a model for the coupled oscillator systems like the diode array. In what follows, we will focus on the case where the uncoupled maps undergo a period-doubling bifurcation at  $\alpha = \alpha^*$ . Without loss of generality, we can take the bifurcation point for the uncoupled maps to occur at  $x=0$ ,  $\alpha^*=0$ . Thus both  $\alpha$  and  $\lambda$  can be considered small parameters.

More specifically, for the local dynamics  $f(x)$  we use the normal form appropriate for (supercritical) period doubling<sup>42</sup>

$$f(x) = (-1 + \alpha)x + \beta x^2 + \gamma x^3 + \dots,$$

where  $\alpha$  is a small parameter, but  $\beta$  and  $\gamma$  are order unity. Meanwhile, we require that the coupling function  $g(x_1, \dots, x_N)$  retains the permutation symmetry relevant to global coupling. In particular, recall that the correct scaling<sup>42</sup> requires that  $\alpha \sim O(x^2)$ ; if we similarly take  $\lambda \sim \alpha \sim O(x^2)$ , then only the terms in  $g$  that are constant or linear in  $x$  contribute:

$$g = \delta + \eta N^{-1} \sum_j x_j,$$

where  $\delta$  and  $\eta$  are coefficients of order unity. The factor of  $N^{-1}$  has been included so that the coupling term remains bounded as  $N$  grows large. This is naturally tied to the global nature of the coupling term; for a finite-range coupling, such as nearest neighbor, no such factor would be necessary. In particular, we note that this scaling ensures that the fully symmetric state is independent of  $N$ .

Thus our model equations become

$$x_k \rightarrow (-1 + \alpha)x_k + \beta x_k^2 + \gamma x_k^3 + \lambda \delta + \lambda \eta N^{-1} \sum_j x_j + O(x_k^4). \quad (2)$$

If this model correctly describes the coupled oscillator array at all, we expect it to do so when both  $\lambda$  and  $\alpha$  are small parameters. Thus our first step is to understand the

basic structure of the uncoupled problem, and then follow the effect of “turning on” the coupling parameter  $\lambda$ .

The uncoupled problem has a fixed point at  $x_k = 0$ , for all parameter values, which corresponds to the in-phase period-one solution. This solution exhibits a bifurcation at  $\alpha = 0$ , beyond which there are  $2^{N-1}$  distinct stable period-2 orbits (in addition to the now unstable period-1 orbit). This multiplicity arises because, relative to  $x_1$ , each oscillator may be either in phase or out of phase with  $x_1$ . (There are, of course, a number of other unstable orbits as well, corresponding to solutions in which any number of the  $x_k$  are zero.) It is convenient to label these many states according to some macroscopic measure. In particular, for a period-2 state in which the  $N$  elements have broken into synchronized groups of  $m$  and  $(N - m)$ , we introduce the “excess”  $\Gamma = 2m - N$ . Consequently, when exactly half of the oscillators are in each phase of the period-two oscillation,  $\Gamma = 0$ . In fact,  $\Gamma$  may be thought of as labeling the symmetry of the different orbits beyond the bifurcation point. Our goal is to follow these orbits when  $\lambda$  is varied away from zero: we find that orbits of different symmetry have different stability ranges.

What are the questions we will try to answer? First, we will look at the *stability ranges* of orbits having different  $\Gamma$ : we will be able to directly compare predictions based on the maps with data from the electrical circuit. This will give us a handle on the degree to which the coupled maps can be taken seriously as a model for the physical system. It also gives us a way to calibrate the map parameters  $\alpha$  and  $\lambda$  with the experimental parameters. We will then turn to a more ambitious problem, which concerns the fact that there are (for large  $N$ ) exponentially many coexisting attractors. In an effort to get a gross handle on the ensuring behavior, we will try to make a connection between the sharing of phase space in the noise-free system with the statistical behavior of the system in the presence of noise. In particular, we will follow the probability of finding the system in a state corresponding to any particular symmetry value  $\Gamma$ , as a function of the local stress parameter  $\alpha$  and the coupling parameter  $\lambda$ .

### III. ANALYSIS OF MODEL

One could begin to study the above model equations as they stand. Moreover, because we are interested in the period-doubled regime, it is easier to study the second iterate of the coupled maps.<sup>42</sup> Applying Eq. (2) twice, the new map equations are

$$x_k \rightarrow (1 - 2\alpha - 2\lambda\beta\delta)x_k - 2(\gamma + \beta^2)x_k^3 - 2\lambda\eta N^{-1} \sum_j x_j + O(x_k^4). \quad (3)$$

By rescaling, this can be written in the following general form:

$$x_k \rightarrow (1 + \mu)x_k - x_k^3 + \frac{\epsilon}{N} \sum_j x_j. \quad (4)$$

The coupled map equations depend on two parameters:

the stress  $\mu$  and the coupling strength  $\epsilon$ . We can calculate the fixed points corresponding to period-2 orbits of the original system, and determine their stability properties. We find that the excess  $\Gamma$  is an important factor in determining the stability of a given solution.

Our first task is to find the fixed points of Eq. (4). It is easy to see what these are for the special case  $\epsilon = 0$ . In this case, below the bifurcation point ( $\mu < 0$ ) there is only the one solution  $x_1 = x_2 = \dots = x_N = 0$ , while above the bifurcation point ( $\mu > 0$ ) we can independently choose  $x_k$  to be any of the three values 0 or  $\pm\sqrt{\mu}$ , so that there are  $3^N$  solutions. It is also clear that all of these latter solutions, which have  $x_k = 0$  for any  $k$ , are saddle points, while the remaining  $2^N$  solutions are stable for some range of  $m$ . In what follows, we are interested in computing these  $2^N$  solutions, and their stability properties, for  $\epsilon \neq 0$ . To do this, we set

$$\begin{aligned} x_j &= x_+, \quad j = 1, 2, \dots, m \\ x_j &= x_-, \quad j = m + 1, \dots, N \end{aligned} \quad (5)$$

so that the oscillator array decomposes into two groups, of size  $m$  and  $N - m$ , respectively. We define  $\Gamma$  for this solution by  $2m - N$ , so that  $\Gamma = 0$  when  $m = N/2$ . The next step is to substitute Eq. (5) into Eq. (4), and solve the resulting algebraic equations

$$\begin{aligned} x_+ &= (1 + \mu)x_+ - x_+^3 + \frac{\epsilon}{N}mx_+ + \frac{\epsilon}{N}(N - m)x_- , \\ x_- &= (1 + \mu)x_- - x_-^3 + \frac{\epsilon}{N}mx_+ + \frac{\epsilon}{N}(N - m)x_- \end{aligned} \quad (6)$$

for  $x_+$  and  $x_-$ . We are interested in the solutions where neither  $x_+$  nor  $x_-$  is zero. For  $\Gamma = 0$  or  $\pm N$  we easily find the exact solutions. The other solutions may also be found in closed form, by introducing the variables  $u = x_+ + x_-$  and  $v = x_+ - x_-$ , which leads to a cubic polynomial in  $u^2$

$$u^6 - (2\mu - \epsilon)u^4 + \frac{1}{4}(2\mu - \epsilon)^2 + 3\left[\frac{\Gamma\epsilon}{N}\right]^2 u^2 - \left[\frac{\Gamma\epsilon}{N}\right]^2 \mu = 0. \quad (7)$$

However, it is more convenient to solve Eqs. (6) by expressing the answer as an expansion in  $\epsilon$ . Sufficient accuracy is obtained by taking the expansion to second order, so that

$$\begin{aligned} x_+ &= \mu^{1/2} + \frac{\epsilon}{2\mu^{1/2}} \frac{\Gamma}{N} + \frac{\epsilon^2}{4\mu^{3/2}} \left[ \frac{\Gamma}{N} - \frac{3}{2} \frac{\Gamma^2}{N^2} \right], \\ x_- &= -\mu^{1/2} + \frac{\epsilon}{2\mu^{1/2}} \frac{\Gamma}{N} + \frac{\epsilon^2}{4\mu^{3/2}} \left[ \frac{\Gamma}{N} + \frac{3}{2} \frac{\Gamma^2}{N^2} \right]. \end{aligned} \quad (8)$$

Of course, Eq. (8) represents a whole multiplet of solutions, wherein any  $m$  of the  $x_k$  are equal to  $x_+$ , and the remaining  $x_k$  are equal to  $x_-$ , so that the multiplet contains  $N!/m!(N - m)!$  symmetry-related solutions.

To determine the stability range of these solutions, we

linearize Eq. (4) about the fixed point Eq. (8). This leads to the matrix equation

$$\eta_k \rightarrow \sum_j M_{kj} \eta_j,$$

where  $\eta_k$  is the deviation of  $x_k$  from its fixed point value, and  $M$  is an  $N \times N$  coefficient matrix. The eigenvalues  $\lambda_i$  of  $M$  determine the stability of the fixed point; stability requires  $|\lambda_i| < 1$  for all  $i$ . Although there are  $N$  eigenvalues in all, the symmetry of the problem allows one to make a transformation that greatly simplifies the analysis. Specifically, one can introduce the following change of variables

$$\Xi = \sum_{j=1}^m \eta_j, \quad \Psi = \sum_{j=m+1}^N \eta_j;$$

$$\xi_k = \eta_k - \eta_{k+1}, \quad k = 1, \dots, m-1;$$

$$\psi_k = \eta_k - \eta_{k+1}, \quad k = m+1, \dots, N-1.$$

This transformation very nearly diagonalizes the linearized problem: the resulting matrix is now reduced to a single  $2 \times 2$  block—corresponding to mixing between  $\Xi$  and  $\Psi$ —and is otherwise diagonal. The symmetry thereby leads to only a small number of distinct eigenvalues: to second order in  $\epsilon$ , these are

$$\begin{aligned} \lambda_1 &= 1 - 2\mu - 3\epsilon \frac{\Gamma}{N} - \frac{3}{2} \frac{\epsilon^2}{\mu} \frac{\Gamma}{N} \left[ 1 - \frac{\Gamma}{N} \right], \\ \lambda_2 &= 1 - 2\mu + 3\epsilon \frac{\Gamma}{N} + \frac{3}{2} \frac{\epsilon^2}{\mu} \frac{\Gamma}{N} \left[ 1 + \frac{\Gamma}{N} \right], \\ \lambda_3 &= 1 - 2\mu + \frac{1}{2}\epsilon(1+\kappa) + \frac{3}{2} \frac{\epsilon^2}{\mu} \left[ \frac{\Gamma}{N} \right]^2 \left[ 1 + \frac{5}{\kappa} \right], \\ \lambda_4 &= 1 - 2\mu + \frac{1}{2}\epsilon(1-\kappa) + \frac{3}{2} \frac{\epsilon^2}{\mu} \left[ \frac{\Gamma}{N} \right]^2 \left[ 1 - \frac{5}{\kappa} \right], \end{aligned} \quad (9)$$

where  $\kappa = (1 + 24\Gamma^2/N^2)^{1/2}$ . The first two eigenvalues correspond to the coordinates  $\xi_k$  and  $\psi_k$ , which have multiplicity  $m-1$  and  $N-m-1$ , respectively. The last two eigenvalues correspond to the remaining  $2 \times 2$  block.

From Eqs. (9), the stability boundaries in the  $\mu$ - $\epsilon$  plane can be determined readily, for any choice of  $\Gamma/N$ . The special case of  $\Gamma = N$  deserves a closer look. When all of the oscillators are in phase, the fixed points are given *exactly* by  $x_+ = \sqrt{\mu + \epsilon}$ . This gives us a check for the stability results based on the second-order expressions, Eqs. (8) and (9), at least for this special case. Although the differences are not critical for small  $N$ , the deviation from the exact results become more substantial for large- $N$  systems. We also note that this state has only two (distinct) eigenvalues, since the simplifying transformation requires only  $\Xi$  and  $\xi_k$ , and not  $\Psi$  and  $\psi_k$ . As we shall see in Sec. IV, this has important consequences for the relative stability of this state, compared with the other period-2 solutions.

More generally, we can compare the analytic expressions for the stability boundaries, for any  $\Gamma$ , with its cor-

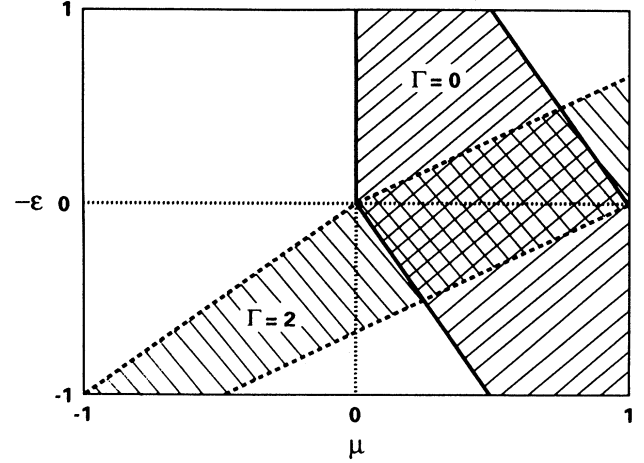


FIG. 2. Analytical stability diagram for  $N=2$ .

responding numerical simulation. The simulation consists of selecting a particular  $\mu$ - $\epsilon$  pair, then inserting a range of initial conditions for the  $\{x_k\}$ . For each set of initial conditions, Eq. (4) is iterated a sufficient number of times until the iterates settle down to an attractor. This attractor is either a steady state corresponding to a particular value of  $\Gamma$ , or some higher period solution. (That is, for some parameter values, fixed point solutions may coexist with other, time-dependent, solutions.) Repeating this procedure yields a stability diagram in the  $\mu$ - $\epsilon$  plane.

In order to get an idea as to how well these approximations can be trusted, we consider the case of  $N=2$ . Figure 2 shows the stability diagram of the map array. On the scale of this figure, the second-order results are virtually indistinguishable from those obtained by direct numerical iteration, suggesting that we can take seriously the analytic expressions given by Eqs. (9). It is somewhat surprising that the agreement extends out to parameter values of order unity for both  $\epsilon$  and  $\mu$ ; this wide range of agreement is possibly fortuitous, but in any event is unimportant for our present purposes. This is because the validity of the iterative map array as a model of real systems, e.g., the circuit array, was predicated on an expansion in terms of the small parameters  $\epsilon$  and  $\mu$ .

#### IV. DYNAMICS OF LARGER ARRAYS

We turn now to the behavior of arrays composed of more than two elements. The resulting dynamical system typically has many coexisting attractors. We focus on two particular issues: the stability ranges of the various period-2 attractors and the competition between these many attractors for available phase space, e.g., the relative sizes of the basins of attraction.

As  $N$  becomes increasingly large, there can be several overlapping regions of  $\Gamma$  stability, i.e., regions over which solutions corresponding to different values of  $\Gamma$  stably coexist. Typically, one finds that for small values of  $\epsilon$ , all period-2 solutions are stable just beyond the onset of the period-doubling bifurcation. As a control parameter is

varied, these solutions lose stability in some order which depends on  $\Gamma$ . Figure 3 compares the analytic and numerical stability limits as a function of  $\epsilon > 0$  for  $N=44$ , when  $\mu=0.5$ . (Note that, quite generally, the stability boundaries of  $\pm\Gamma$  solutions are identical; for convenience we only quote those for positive  $\Gamma$ .)

With one exception, the stability range is a decreasing function of  $\Gamma$ —that is, states corresponding to two groups of nearly equal number have a greater range of stability than states dominated by one phase. Thus, for this sign of coupling the dynamics selects against large-scale synchronization of the array.

There is an exception to this rule: strikingly, it is the extreme case in which *all* of the oscillators are synchronized. Mathematically, the reason for this is that the eigenvalue responsible for the instability for all the other  $\Gamma$  solutions does not exist for the case of  $m=N$  [cf. the discussion following Eq. (9)]. Consequently, the bifurcation of this exceptional solution is fundamentally different than the others. This behavior is especially noteworthy since, in most applications of oscillator arrays, one is interested in stabilizing the solution with the greatest degree of synchronization. In this sense, the exceptional stability of the fully synchronized solution is especially welcome.

While an understanding of the stability limits can be useful in determining when each of the different  $\Gamma$  solutions will be directly observable, it says nothing about the relative probability of finding the system in an orbit corresponding to a particular  $\Gamma$ . For given values of stress and coupling where solutions corresponding to several (and possibly all) values of  $\Gamma$  are stable, we now ask the following: which solutions are most probable? On the face of it, this is a complicated theoretical issue, since the answer depends on both the multiplicity of solutions for a given  $\Gamma$ , the size of the basins of attraction, and the relaxation rate of the dynamics in the vicinity of each attractor. While the multiplicity is easily determined by simple

combinatoric considerations, determining the basin sizes is far more difficult. On the other hand, the relative probabilities are readily determined numerically by searching the  $N$ -dimensional space of initial conditions  $\{x_k\}$  and iterating the coupled map equations. In this way, a measure of the basin size of corresponding to each value of  $\Gamma$  is found as a function of  $\mu$  and  $\epsilon$ .

The numerical results showing basin size versus  $\epsilon$  for  $N=4$  are depicted in Fig. 4. The most noticeable feature is that the more negative  $\epsilon$  value tends to favor the  $\Gamma=0$  states; that is, tends to favor the equal distribution of oscillator phases. Meanwhile, increasingly positive values of  $\epsilon$  tend to force all oscillators into the same phase, corresponding to the  $|\Gamma|=4$  states.

Finally, we turn to numerical simulations for  $N=44$ , which reveal an interesting and unexpected feature. The results for the relative basin size are depicted in Fig. 5, for the extreme cases  $\Gamma=0$  and  $|\Gamma|=44$ , only. As for the smaller array, the evenly divided solutions  $\Gamma=0$  suffer a gradual decrease in their share of the phase space, as  $\epsilon$  increases. On the other hand, the relative basin size of the completely in-phase solution is utterly negligible, except in a narrow range of coupling strength  $\epsilon$ , where its share reaches fully 10% of the available phase space. Recalling that there are 473 of the  $\Gamma=0$  period-2 solutions in all, as compared with only one  $|\Gamma|=44$  solution, it is surprising that the in-phase attractor is observed with any non-negligible weight at all. The narrowness of this peak is also unexpected, insofar as the in-phase states are stable for all  $\epsilon$  down to zero.

The origin of this effect can be understood by correlating this with the stability results of Fig. 3. While the gradual decline for  $\Gamma=0$  is due to an actual shrinking of the size of the individual basins of attraction, the growth for  $|\Gamma|=44$  is due to successive instabilities of the intermediate  $\Gamma$  orbits. As an instability point is approached, the basins do not diminish to zero; rather, a substantial volume of phase space is “orphaned” at the bifurcation

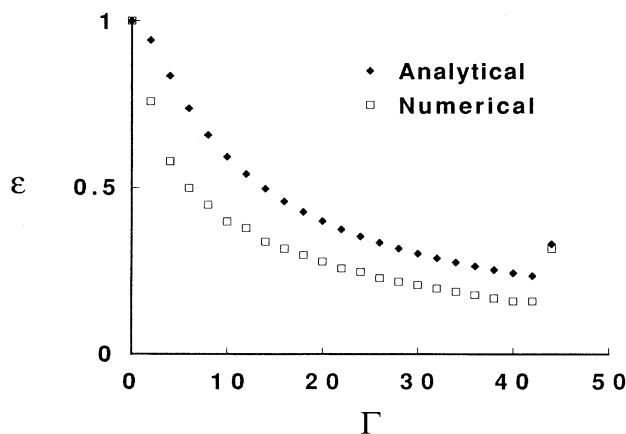


FIG. 3. Upper stability boundary in  $\epsilon$  for different solutions, labeled by excess  $\Gamma$ , for  $N=44$  and  $\mu=0.5$ . The solid symbols represent the second-order result deduced from Eq. (9); the open symbols represent direct numerical iteration of the model map Eq. (4).

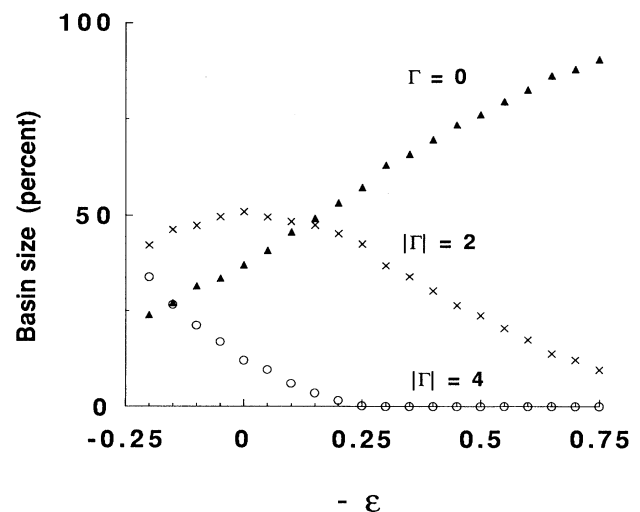


FIG. 4. Relative probability of finding the map array in a period-2 orbit of a given  $\Gamma$ , as a function of  $-\epsilon$ ;  $N=4$ ,  $\mu=0.5$ .

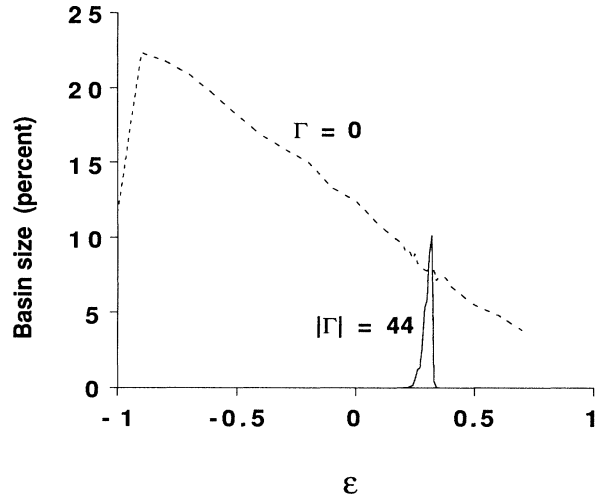


FIG. 5. Relative probabilities of finding the map array in the period-2 orbits  $\Gamma=0$  and 44 as a function of  $\epsilon$ ;  $N=44$ ,  $\mu=0.5$ .

point, and one finds that this volume is always added to the  $|\Gamma|=44$  basin. A close look at Fig. 5 reveals the discrete jumps in the  $|\Gamma|=44$  curve as it increases. Of course, this basin size suddenly drops to zero at its own point of instability.

#### V. EXPERIMENTAL REALIZATION OF A GLOBALLY COUPLED SYSTEM

We return now to the experimental realization of a globally coupled oscillator array, shown in Fig. 1. The particular nonlinear circuit studied here has been well characterized in its single oscillator form.<sup>39–41</sup>

The coupled differential equations describing the multiple oscillator circuit can be written in the following general form:

$$L \frac{dI_j}{dt} = V_s \sin \omega t - RI_j - V_j - R_c \sum_{k=1}^N I_k, \quad (10)$$

$$\frac{dV_j}{dt} = f(I_j, t), \quad j=1, 2, \dots, N \quad (11)$$

where  $I_j$  and  $V_j$  are the current and voltage of the  $j$ th junction,  $L$  is the series inductance,  $R$  is the series resistance,  $V_s$  is the driving voltage amplitude,  $\omega$  is the driving frequency, and  $R_c$  is the coupling resistance. The specific functional relationship between the junction current and voltage, Eq. (11), depends on the particular diode model chosen. Good agreement with experimental results has been achieved for  $N=1$  and 2 by numerically integrating these equations,<sup>43</sup> but this approach becomes less practical for large  $N$ .

Consider first the case of a single oscillator. For low driving voltages, the circuit responds nearly sinusoidally, oscillating at the drive frequency. As the amplitude of the driving voltage is increased, a succession of period-doubling bifurcations will occur, eventually leading to chaos.<sup>39–41</sup> The case of two coupled oscillators behaves

somewhat differently.<sup>8</sup> As the drive amplitude is increased from a low value, the circuit initially experiences a single period doubling; however, depending on the driving frequency, it can then undergo a Hopf bifurcation, leading to quasiperiodic oscillations. Thereafter, still other instabilities are observed. For the purposes of the present work, we will restrict ourselves to a parameter regime where only the first period-doubling bifurcation is relevant; consequently, secondary instabilities such as the Hopf bifurcation will not be a factor.

For reasons of theoretical convenience, one would like to construct the coupled circuit with  $N$  identical resonators. Obviously, this is not possible in a strict sense; nevertheless, without too much trouble one can find reasonably matched elements, to within about 10% variation. This spread in parameters did not prove to be critical to the experimental results, and the circuit's behavior seemed well described by equations that treat the elements as identical.

Although the performance of the coupled circuit depends on several parameters, we will focus on the effects of the coupling resistance  $R_c$  and the driving amplitude  $V_s$ . The other parameters will be fixed so that the first period-doubling region is accessible. In particular, we can identify the quantity  $V_s$  as a "local stress" parameter which drives a single element through an instability, and the quantity  $R_c$  as a "global coupling" parameter which governs the strength of the interaction between elements (so that  $R_c=0$  recovers the uncoupled problem).

In order to test most fully the correspondence between the circuit and the iterative map model, it is handy to have both "positive" and "negative" coupling. In principle, this requires that the coupling resistance  $R_c$  can take on both positive or negative values. In our experiments, the case of negative resistance is achieved by replacing the coupling resistor with a negative impedance converter (NIC). The NIC is an operational amplifier circuit<sup>44</sup> which changes the impedance  $Z$  seen by the remainder of the circuit into an equivalent impedance of  $-Z$ .

Figure 6 shows the results of measurements on the

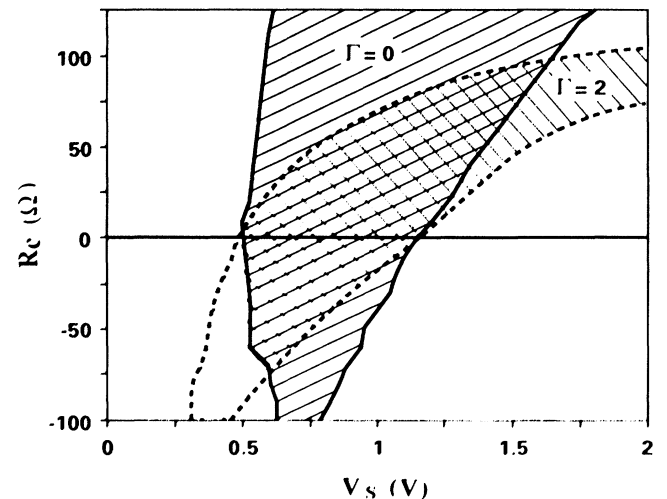


FIG. 6. Experimental stability diagram for  $N=2$ .

diode circuit for  $N=2$ . The general form of the two stability regions  $\Gamma=0$  and 2, as well as their relationship to each other, bears a qualitative similarity to Fig. 2. Consider first the case of a small positive resistance  $R_c$ . As the drive voltage  $V_s$  is increased from zero past the bifurcation point, the circuit period doubles into the out-of-phase  $\Gamma=0$  orbit, as this is the only stable orbit. If the coupling resistance is instead small and negative, as  $V_s$  is increased from zero the circuit period doubles into the in-phase  $\Gamma=2$  orbit at a driving voltage less than the uncoupled bifurcation point  $V_0$ .

Stability diagrams can also be constructed for larger- $N$  circuits. However, we turn instead to the statistical measure introduced in Sec. IV, examples of which are depicted in Figs. 4 and 5. This description, based on the relative probability of finding the array in a particular "macroscopic state," seems to us a more natural way of quantifying systems containing very large numbers of oscillators, or, alternatively, systems where it is not feasible to monitor each degree of freedom separately.

Theoretically, we focused on the total size of the basins of attraction corresponding to a given  $\Gamma$ . In our circuit it is not possible to set arbitrary initial values for current and voltage. However, we can simulate this situation by applying an uncorrelated noise source to each of the individual oscillators. This noise is turned on and off, and the final state of the circuit is observed. Repeating this measurement will produce the basin size information. Although  $N$  independent noise sources should be employed, as a practical matter one noise source is sufficient if a relative time delay in the noise signal greater than the correlation time of the noise is introduced between oscillators, as shown in Fig. 7. This is a cheap and efficient way to ensure that the instantaneous noise in any oscillator is uncorrelated with the noise in any other oscillator.

Figure 8 shows the total basin size corresponding to different values of  $|\Gamma|$  as a function of  $R_c$  for the circuit with  $N=4$ . Note that the sum of the basin sizes add up to 100%, since there are no other attractors in this pa-

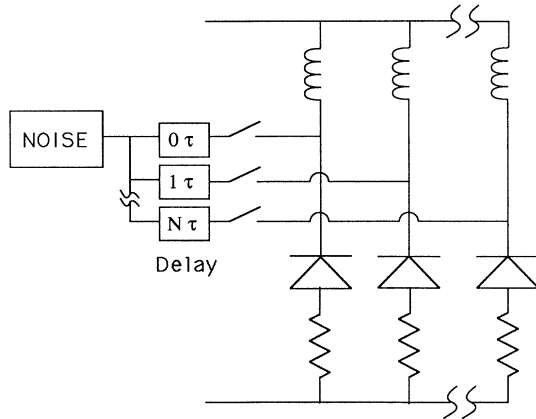


FIG. 7. Schematic of circuit with noise added to array, to sample a range of initial conditions, using a Micronetics noise module ( $V_{rms} = 1.0$  V, noise correlation time less than 10 ns) and circuit delay time  $\tau = 200$  ns.

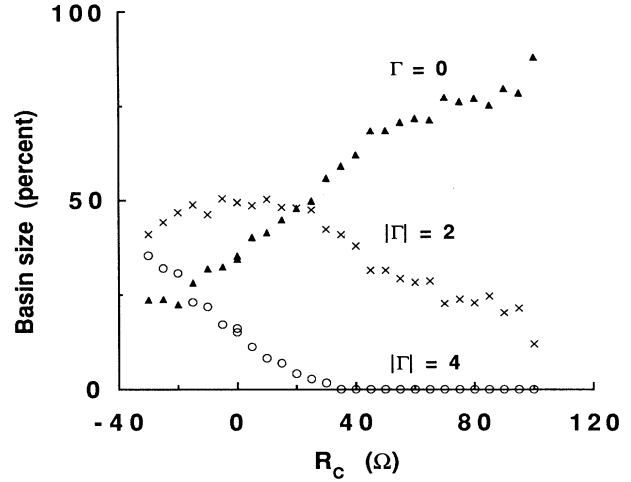


FIG. 8. Relative probability of finding the circuit in a period-2 orbit of a given  $\Gamma$ , as a function of  $R_c$ ;  $N=4$ ,  $V_s = 1.0$  V.

rameter regime. In order to find the basin size per attractor, one should divide by the multiplicity for that value of  $|\Gamma|$ . We chose to monitor the total basin size, since it is most relevant to the measurement of some bulk (or macroscopic) quantity associated with the array, e.g., the total current.

## VI. COMPARISON BETWEEN EXPERIMENT AND THEORY

To compare the behavior of the coupled map equations with the behavior of the circuit, we need to make a connection between the map parameters  $\mu$  and  $\epsilon$  and the circuit parameters  $V_s$  and  $R_c$ . As a general proposition,  $\mu$  and  $\epsilon$  should be expressed as functions of both  $V_s$  and  $R_c$ ; however, we will approximate the map stress  $\mu$  as a function only of the circuit stress  $V_s$ , and the map coupling  $\epsilon$  as a function of the circuit coupling  $R_c$ :

$$\mu = F(V_s),$$

$$\epsilon = G(R_c).$$

We expect that this is a reasonable approximation, based on physical grounds: indeed, our map model was motivated by the distinct roles played by the local stress and the global coupling parameters.

For the uncoupled maps, the period-2 bifurcation point occurs at  $\mu=0$ . If we let  $V_0$  be the driving voltage at the circuit's corresponding bifurcation, then  $\mu$  can be written as

$$\mu = \sum_{j=0}^{\infty} c_j (V_s - V_0)^j,$$

where the coefficients are such that  $V_s > V_0$  for  $\mu > 0$ . In a similar manner, one can express  $\epsilon$  as an expansion in  $R_c$ . The sign of  $\epsilon$  relative to  $R_c$  is crucial: does  $R_c > 0$  correspond to positive or negative  $\epsilon$ ? This can be determined by comparing numerical and experimental stabi-

ty plots for two oscillators as depicted in Figs. 2 and 6.

As noted in Sec. V, the circuit data of Fig. 6 enjoy only a qualitative similarity to the map predictions of Fig. 2. Note, however, that Fig. 6 shows the raw data, without any attempt to scale the experimental parameters  $V_s$  and  $R_c$  to the corresponding model parameters  $\epsilon$  and  $\mu$ . Naturally, such scaling leads to better agreement; however, for our purposes we are not interested in establishing detailed quantitative correspondence between the experiment and the model iterative maps.

More specifically, a basic similarity of behavior can be seen if  $R_c$  is identified with  $-\epsilon$ . Thus a small negative  $\epsilon$  first will produce a  $\Gamma=0$  orbit when  $\mu$  is increased past zero, while a small positive  $\epsilon$  will produce first a  $\Gamma=2$  orbit while  $\mu$  is still negative. Therefore a positive value of  $\epsilon$  shifts the bifurcation point to a lower value of stress  $\mu$ , just as a negative value of  $R_c$  does for the circuit. The foregoing suggests that we have, for small  $\epsilon$

$$\epsilon = -aR_c,$$

where  $a$  is a positive constant.

Of greater interest is the case  $N > 2$ , to which we now turn. We compare the basin size computation for the map array (Fig. 4), with the randomly perturbed circuit measurements (Fig. 8). Recall that negative values of  $\epsilon$  correspond to positive values of  $R_c$ . The figures indicate that the map model predicts the dynamical response of the circuit quite well. In particular, we see that positive  $R_c$  (negative  $\epsilon$ ) tends to more evenly distribute the relative phases between oscillators (lower  $|\Gamma|$ ), while negative  $R_c$  (positive  $\epsilon$ ) tends to force greater synchronization of the group as a whole (higher  $|\Gamma|$ ).

The correspondence between the map model and the experimental results was quite good for  $N=2, 3$ , and 4, even without scaling the stress parameters  $\mu$  and  $V_s$ . Although the stability limits depend substantially on  $\mu$  and  $V_s$ , we find that the basin sizes are not greatly affected as the stress is varied within a stability range. Rather, it is the coupling term which plays the greater role in determining basin size.

## VII. SUMMARY AND CONCLUSIONS

In this paper, we have investigated a specific example of a feature common in oscillator arrays, namely the appearance of large numbers of coexisting attractors. A

simple yet useful picture of the systems studied is that they consist of local degrees of freedom—controlled to a local stress parameter—subject to a coupling between degrees of freedom, whose strength is independently controlled. The coupling studied was global, in which all oscillators are coupled to all others, with equal strength. Such coupling occurs in both electrical circuits and multimode laser systems: here we constructed a parallel array of  $p$ - $n$  junction diode oscillators, though of fairly small size, up to  $N=4$ . In addition, we introduced a set of coupled iterated maps, which enabled us to understand certain features of the circuit array, and also allowed us to consider (numerically) the behavior of much larger arrays.

We focused on the vicinity of a single period-doubling bifurcation point, for which the system can have as many as  $2N-1$  coexisting periodic attractors. Inevitably, with so many coexisting states, one is led to consider some kind of statistical description of the dynamical system. We found it convenient to label certain classes of attractors according to their symmetry, or (what amounts to the same thing here) their degree of synchronization. A combination of straightforward linear stability analysis, together with measurements of the relative sizes of the various basins of attraction, revealed some interesting and understandable behavior. Of particular interest are some circumstances that especially favor the completely in-phase solution: for example, for  $N=44$ , we find this state can attract fully 10% of all initial conditions. This is somewhat unexpected insofar as this occurs when it coexists with 473 other stable periodic orbits.

In fact, it is possible to choose the parameters  $\mu$  and  $\epsilon$  such that the completely in-phase period-2 solution is the only stable solution. That is, not only are all of the other period-2 solutions unstable, but there are no attractors of any other type. The in-phase state is therefore globally attracting—that is, its basin occupies 100% of the phase space.

## ACKNOWLEDGMENTS

We thank Rajarshi Roy and James W. Swift for valuable discussions. The comments of Charles Braden on the experimental aspects were especially helpful. L.F. acknowledges support from the National Science Foundation; K.W. was supported by the Office of Naval Research.

<sup>1</sup>T. Hogg and B. A. Huberman, Phys. Rev. A **29**, 275 (1984).

<sup>2</sup>K. Kaneko, Prog. Theor. Phys. **69**, 1427 (1983).

<sup>3</sup>J.-M. Mao and R. H. Helleman, Phys. Rev. A **35**, 1847 (1987).

<sup>4</sup>P. Hadley and M. R. Beasley, Appl. Phys. Lett. **50**, 621 (1987).

<sup>5</sup>Z. Su, R. W. Rollins, and E. R. Hunt, Phys. Rev. A **40**, 2689 (1989).

<sup>6</sup>P. S. Linsay and A. W. Cumming, Phys. Rev. Lett. **60**, 2719 (1988).

<sup>7</sup>P. S. Linsay and A. W. Cumming, Physica D **40**, 196 (1989).

<sup>8</sup>R. van Buskirk and C. Jeffries, Phys. Rev. A **31**, 3332 (1985).

<sup>9</sup>J. Shrager, T. Hogg, and B. A. Huberman, Science **236**, 1092 (1987).

<sup>10</sup>T. Bohr, G. Grinstein, Yu He, and C. Jayaprakash, Phys. Rev. Lett. **58**, 2155 (1987).

<sup>11</sup>J. P. Crutchfield and K. Kaneko, in *Directions in Chaos Vol. I*, edited by B.-L. Hao (World Scientific, Singapore, 1987).

<sup>12</sup>J. P. Crutchfield and K. Kaneko, Phys. Rev. Lett. **60**, 2715 (1988).

<sup>13</sup>P. Alstrom and R. K. Ritala, Phys. Rev. A **35**, 300 (1987).

<sup>14</sup>S. N. Coppersmith and P. B. Littlewood, Phys. Rev. Lett. **57**, 1927 (1986).

<sup>15</sup>S. N. Coppersmith and P. B. Littlewood, Phys. Rev. B **36**, 311 (1987).

<sup>16</sup>C. Tang, K. Wiesenfeld, P. Bak, S. Coppersmith, and P. B.



- Littlewood, Phys. Rev. Lett. **58**, 1161 (1987).
- <sup>17</sup>S. S. Wang and H. G. Winful, Appl. Phys. Lett. **52**, 1774 (1988).
- <sup>18</sup>C. M. Marcus, S. H. Strogatz, and R. M. Westervelt, Phys. Rev. B **40**, 5588 (1989).
- <sup>19</sup>S. H. Strogatz and R. M. Mirollo, Physica D **31**, 143 (1988).
- <sup>20</sup>S. H. Strogatz and R. M. Mirollo, J. Phys. A **21**, L699 (1988).
- <sup>21</sup>E. Fermi, J. R. Pasta, and S. Ulam, Los Alamos Report No. LA-1940, 1955; also in *Collected Works of Enrico Fermi* (University of Chicago Press, Chicago, 1965), Vol. 2, p. 978.
- <sup>22</sup>G. L. Oppo and R. Kapral, Phys. Rev. A **36**, 5820 (1987).
- <sup>23</sup>I. Waller and R. Kapral, Phys. Rev. A **30**, 2047 (1984).
- <sup>24</sup>J. D. Keeler and J. D. Farmer, Physica D **23**, 415 (1988).
- <sup>25</sup>D. K. Umberger, C. Grebogi, E. Ott, and B. Afeyan, Phys. Rev. A **39**, 4835 (1989).
- <sup>26</sup>P. Hadley, M. R. Beasley, and K. Wiesenfeld, Phys. Rev. B **38**, 8712 (1988).
- <sup>27</sup>K. Wiesenfeld and P. Hadley, Phys. Rev. Lett. **62**, 1335 (1989).
- <sup>28</sup>K. Y. Tsang and K. Wiesenfeld, Appl. Phys. Lett. **56**, 495 (1990).
- <sup>29</sup>P. Bak, C. Tang, and K. Wiesenfeld, Phys. Rev. Lett. **59**, 381 (1987); Phys. Rev. A **38**, 364 (1988).
- <sup>30</sup>K. Wiesenfeld, C. Tang, and P. Bak, J. Stat. Phys. **54**, 1441 (1989).
- <sup>31</sup>P. Bak and C. Tang, Phys. Today **42**, S27 (1989).
- <sup>32</sup>B. A. Huberman and T. Hogg, Phys. Rev. Lett. **52**, 1048 (1984).
- <sup>33</sup>B. A. Huberman and T. Hogg, U. S. Patent No. 4,591,980, May 27, 1986.
- <sup>34</sup>K. Kaneko, Physica D **41**, 137 (1990).
- <sup>35</sup>G. E. James, Ph.D. dissertation, Georgia Institute of Technology, 1990 (unpublished).
- <sup>36</sup>G. E. James, E. Harrell II, and R. Roy, Phys. Rev. A **41**, 2778 (1990).
- <sup>37</sup>*Multiparameter Bifurcation Theory*, Vol. 56 of *Contemporary Mathematics*, edited by M. Golubitsky and J. Guckenheimer (American Mathematical Society, Providence, 1986).
- <sup>38</sup>M. Golubitsky and D. G. Schaeffer, *Singularities and Groups in Bifurcation Theory* (Springer-Verlag, New York, 1985).
- <sup>39</sup>P. S. Linsay, Phys. Rev. Lett. **47**, 1349 (1981).
- <sup>40</sup>J. Testa, J. Perez, and C. Jeffries, Phys. Rev. Lett. **48**, 714 (1982).
- <sup>41</sup>R. W. Rollins and E. R. Hunt, Phys. Rev. Lett. **49**, 1295 (1982).
- <sup>42</sup>J. Guckenheimer and P. Holmes, *Nonlinear Oscillations, Dynamical Systems and Bifurcations of Vector Fields* (Springer, New York, 1981), Chap. 3.
- <sup>43</sup>Z. Su, R. W. Rollins, and E. R. Hunt, Phys. Rev. A **40**, 2698 (1989).
- <sup>44</sup>P. Horowitz and W. Hill, *The Art of Electronics* (Cambridge University Press, Cambridge, England, 1989).